Heliyon 10 (2024) e29822

Contents lists available at ScienceDirect

Heliyon

journal homepage: www.cell.com/heliyon

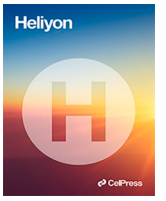

Research article

Numerical exploration of multi-octave spanned supercontinuum generation with high coherence in single material photonic crystal fiber

Shah Md Salimullah [a,b,*], Mohammad Faisal [a]

[a] Department of Electrical and Electronic Engineering, Bangladesh University of Engineering and Technology, Dhaka 1000, Bangladesh
[b] Department of Electrical and Electronic Engineering, Ahsanullah University of Science and Technology, Dhaka 1208, Bangladesh

ARTICLE INFO

Keywords:
Zinc–germanium diphosphide
Photonic crystal fiber
Supercontinuum generation

ABSTRACT

We propose a single material microstructured optical fiber with more than five octave spanning supercontinuum generation. Due to using single material, compatibility checking between core and cladding material need not required. Moreover, the material is such chosen that optical transmission range is quite high in comparison to others. The fiber is designed in COMSOL platform and according to finite element method (FEM), numerical analysis is accomplished. Dispersion, confinement loss, nonlinearity etc. are investigated and exposed for a wavelength range of 2000–3000 nm. The proposed fiber reveals zero dispersion at 2200 nm, nonlinearity of 14,370 $W^{-1}km^{-1}$ and confinement loss around 10^{-9} order in dB/m. Finally, supercontinuum generation has been investigated inside the structure and obtained high coherence that span (from 1500 nm to 34,500 nm) over five octave. The generated spectrum fulfills the requirements for being applicable in frequency metrology, fiber laser and biophotonics. With the best of our knowing, such coherent and widened supercontinuua for single material fiber is yet to be proposed.

1. Introduction

Supercontinuum (SC) is the continuum generated when short pulses with high power interacts nonlinear phenomena during propagation inside an optical fiber. It was first witnessed in 1970 by two person named Shapiro and Alfano [1]. This continuum belongs to a wide range of applications in telecommunication [2], optical frequency metrology [3], molecular spectroscopy [4], optical coherence tomography [5], optical frequency comb generation [6], biomedical purposes [7] etc.

Essentially, when a laser emits an optical pulse and it travels through a highly nonlinear medium such as Photonic Crystal Fiber (PCF), it results in the generation of a broad spectrum of light known as wideband SC. Silica [8], ZBLAN [9], chalcogenides [10–14], tellurite [15,16] based PCFs have been investigated both numerically and experimentally in this regard. Although silica fibers effectively confine light, they exhibit significant absorption beyond the wavelength of 2200 nm which affects the SC spectra to get widened. ZBLAN and tellurite fibers are adequately capable of achieving SC when exposed to light. Again these fibers suffer from significant propagation losses. Therefore, materials with higher refractive indices, wider transmission windows and lower absorption

* Corresponding author. Department of Electrical and Electronic Engineering, Bangladesh University of Engineering and Technology, Dhaka 1000, Bangladesh.
E-mail addresses: sm.salimullah.eee@aust.edu, saikateee07@gmail.com (S.M. Salimullah).

https://doi.org/10.1016/j.heliyon.2024.e29822
Received 26 December 2023; Received in revised form 15 April 2024; Accepted 16 April 2024
Available online 16 April 2024

are more suitable for achieving wideband supercontinua. On the above context, $ZnGeP_2$ can perform better as it has large refractive index, wider transmission window as of 700 nm–13,000 nm [17,18] and presents 5.4×10^{-18} m^2/W [19] kerr nonlinear coefficient. Besides, this material exhibits zero absorption [17,19] beyond 2000 nm.

Recently, numerous theoretical and experimental findings are revealed regarding SC generation in single and multi-material PCF. An experimental study [20] demonstrates a fiber for SC generation whose span is marked as 1070–2310 nm and 890–2460 nm. For 70 fs input, 1800 nm spanned SC has been achieved in lead-bismuth-gallate oxide PCF which has been fabricated by Klimczak et al. [21]. However, the span covered is not well enough. A researcher reported [11] 9000 nm spanned SC spectra in single material PCF ($GeSe_2$-As_2Se_3–PbSe). The scholar has further improved the findings and reported in other study with improved nonlinearity of 991 $W^{-1}km^{-1}$ [14]. Recently, Shakhawath et al. [13] has investigated $Ge_{20}Sb_{15}Se_{65}$ based PCF and projected SC generation at 3900 and 4500 nm. Kalra et al. [22] presented composite PCF (As_2S_3 and borosilicate) for mid-infrared SC generation where they achieved 2100 nm long continuum. The analysis of the coherence of SC spectra was absent in their study. Another composite fiber with silicon core and MgF_2 cladding has been reported [23] for SC generation of about 2670 nm spanning. However, the spectral bandwidth achieved is not worthy enough in comparison to other composite PCF. A bit improved SC spanning (2996 nm) has been introduced [24] through Si_3N_4 based waveguide. But they used silica and due to high absorption loss, less spectral widening achieved in SC. Another researcher [25] addressed this shortcomings by replacing silica with MgF_2 and reported better findings of SC bandwidth as 5700 nm. However, regarding the coherence of the spectrum, they have said nothing. In a subsequent investigation, Karim et al. [26] suggested silicon-rich silicon nitride waveguide to achieve SC with high coherence. Their research resulted in a wide spectrum spanning 6300 nm. However, the scope for engineering the dispersion profile was found inadequate. To attain enlarged spectrum, the dispersion is desired to be tuned to select pump wavelength in the vicinity to zero dispersion wavelength (ZDW). Hence the scholars are contributing relentlessly to find the best suited optical properties for single material PCF [9,11,13] and coherent SC generation as well.

In this study, a simple structure single material PCF has been revealed for multi octave SC generation. The fiber is such designed (large air hole diameter) that it will not face fabrication difficulties, core and cladding material compatibility, large light transmission window and so on. The fiber exhibits ZDW at 2200 nm, high nonlinearity near ZDW as of 14,370 $W^{-1}km^{-1}$ and low confinement loss of 10^{-9} dB/m. Around more than five octave spanning (from 1500 nm to 34,500 nm) SC is obtained numerically through 1 mm of the proposed fiber. As mentioned earlier, the fabrication of such a design does not pose any challenges, as advancements in technology have already allowed researchers to fabrication [27,28] with diameters significantly smaller than the proposed one.

2. Proposed geometrical design and fabrication details

The proposed design features a five-layer configuration of air holes, each with a diameter (d) of 2 μm, as depicted in Fig. 1(a). Fig. 1 (b) illustrates the distribution of the electric field within the fiber. This arrangement of air holes significantly influences material loss and offers distinct advantages [15]. The pitch, denoted by Λ, between adjacent air holes from the center is 3 μm. Fig. 1 (b) illustrates the electric field distribution within the fiber. The refractive index (n) variation of the chosen background material ($ZnGeP_2$) with wavelength (λ) can be described by the Sellmeier equation [18]:

$$n^2 - 1 = 4.67491 + \frac{4.077926\lambda^2}{\lambda^2 - 0.159328} + \frac{1.896005\lambda^2}{\lambda^2 - 900} \tag{1}$$

As the material we have selected has crystalline structure hence fabrication of fiber from such material is of a great concern. Two primary methods, namely micro – pulling down (μ-PD) and laser-heated pedestal growth (LHPG), stand out as the main techniques for growing single crystal fibers. Diverse growth techniques exist for single crystal fibers, but these two methods hold particular significance. For fabricating PCF with diameter in micrometer range, LHPG technique is most favorable. The process begins with the

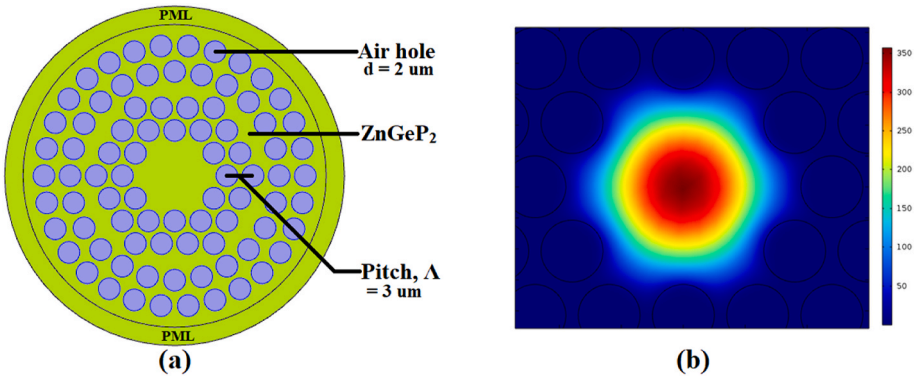

Fig. 1. (a) Graphic cross-sectional figure of designed single material ($ZnGeP_2$) fiber with specification as Λ = 3 μm and d = 2 μm. Core is presented in an enlarged look; (b) Electric field profile with power level indicated color bar. (For interpretation of the references to color in this figure legend, the reader is referred to the Web version of this article.)

preparation of a suitable starting material. Typically, a solid rod or preform of the desired crystal material is used. A small portion of the preform is melted using a high-power laser beam. The molten material forms a small droplet or pedestal, which serves as the seed for crystal growth. The pedestal is formed by carefully adjusting the laser power and positioning to achieve controlled melting. Once the pedestal is formed, the preform is slowly and precisely pulled away from the molten zone. The surface tension of the molten material causes it to elongate and form a fiber-like structure. As the fiber is pulled, it solidifies and crystal growth occurs along its length. The laser beam is continuously focused on the melting zone, maintaining it at a temperature above the material's melting point. This localized heating prevents the solidification of the molten material, allowing for controlled crystal growth. The laser power and scanning speed are carefully adjusted to regulate the growth rate and maintain uniformity. The diameter of the resulting single crystal fiber can be controlled by adjusting the pulling speed and laser power. Slower pulling speeds and higher laser powers generally lead to thicker fibers, while faster pulling speeds and lower laser powers result in thinner fibers. Once the desired length of the crystal fiber is achieved, the pulling process is stopped, and the fiber is cooled gradually to room temperature. Annealing processes may follow to relieve any residual stress and improve the crystal quality.

3. Mathematical interpretation of linear and nonlinear features

For realizing broad continuum generation numerically, short pulse propagation along our structure is investigated through the following generalized nonlinear Schrödinger equation (GNLSE) [15]:

$$\frac{\partial A}{\partial z}+\frac{1}{2}\alpha A-\left(\sum_{k\geq 2}\beta_k\frac{i^{k+1}}{k!}\frac{\partial^k A}{\partial T^k}\right)=i\gamma\left(1+i\frac{1}{\omega_0}\frac{\partial}{\partial T}\right)\times\left[A(z,T)\int_{-\infty}^{\infty}R(T')|A(z,T-T')|^2dT'\right]. \tag{2}$$

$A(z, T)$ indicates altering field envelope, where T symbolizes group velocity oriented time frame ($T = t - \beta_1 z$). β_k refers dispersion parameter of k-th order. Here, α, ω_0 and γ stands for fiber loss, central frequency and nonlinearity respectively. Nonlinearity can be obtained from the following equation,

$$\gamma=\left(\frac{2\pi n_2}{\lambda A_{eff}}\right), \tag{3}$$

Where, n_2 depicts nonlinear refractive coefficient. A_{eff} symbolizes effective modal area and can be estimated by complex electric field, E:

$$A_{eff}=\frac{\left(\iint|E|^2dxdy\right)^2}{\left(\iint|E|^4dxdy\right)}, \tag{4}$$

The function $R(T)$ of material has been incorporated in Eq. (2) as:

$$R(T)=(1-f_R)\delta(T)+f_R h_R(T), \tag{5}$$

f_R, $\delta(T)$ and $h_R(T)$ refers Raman effect, delta function and delayed Raman impact respectively. $h_R(t)$ is obtained from the following equation:

$$h_R(t)=\left(\frac{{\tau_1}^2+{\tau_2}^2}{\tau_1{\tau_2}^2}\right)\exp\left(-t/\tau_2\right)\sin\left(t/\tau_1\right), \tag{6}$$

Where τ_1 indicates Raman period and τ_2 denotes damping time. Like various similar materials [15,29] in the context of refractive index, f_R, τ_1 and τ_2 are considered as of 0.031, 15.5 fs and 230.5 fs for our proposed one. Pulse propagation dynamics is observed by solving GNLSE according to Split-step Fourier method (SSFM) considering the following input,

$$A(z=0,T)=\sqrt{P_0}sech\left(\frac{T}{T_0}\right) \tag{7}$$

Where T_0 denotes pulse width and P_0 is maximum power. For normalizing the GNLSE some variables assumed as,

$$u=\frac{A}{\sqrt{P_0}},\xi=\frac{z}{L_D},\tau=\frac{T}{T_0}, \tag{8}$$

Here $L_D = T_0^2/|\beta_2|$ denotes the fiber length with dominant second order dispersion and GNLSE forms the following format:

$$\frac{\partial u}{\partial\xi}+i\frac{1}{2}\frac{\partial^2 u}{\partial\tau^2}=iN^2\left(1+is\frac{\partial}{\partial\tau}\right)\left[u(\xi,\tau)\int_{-\infty}^{\infty}R(\acute{\tau})|u(\xi,\tau-\acute{\tau})|^2d\acute{\tau}\right] \tag{9}$$

Here, $N^2 = \gamma P_0 T_0^2/|\beta_2|$ describes order of soliton and $s = 1/(\omega_0 T_0)$ indicates self-steepening factor. Fiber attenuation loss has been ignored since the fiber length of our proposed study is short.

Large nonlinearity and small dispersion are greatly desired to obtain broad continuum in a fiber. Our proposed structure is engineered to fulfill the desire. Dispersion, D comprises material dispersion(D_{mat}) and waveguide dispersion (D_{wave}) and obtained from the propagation constant which is given by,

$$D = D_{mat} + D_{wave}$$

$$= -2\pi c \frac{\beta_2}{\lambda^2}$$

$$= -\frac{\lambda}{c} \frac{\partial^2 \mathrm{Re}\left(n_{eff}(\lambda)\right)}{\partial \lambda^2} \tag{10}$$

Second, third, fourth up to tenth order dispersion has been considered in this study and all these are achieved from Taylor's series expansion as follows:

$$\beta(\omega_0) = \beta_0 + \beta_1(\omega - \omega_0) + \frac{1}{2!}\beta_2(\omega - \omega_0)^2 + \frac{1}{3!}\beta_3(\omega - \omega_0)^3 + \ldots \tag{11}$$

The kth order terms as generalized one can be written as

$$\beta_k = \left.\frac{d^k \beta}{d\omega^k}\right|_{\omega=\omega_0}$$

Another significant parameter, confinement loss (CL) has great impact in selecting fiber as it has a close relation in tuning nonlinearity property. CL is estimated from following

$$CL(\lambda) = 8.686 \times \frac{2\pi}{\lambda} \times \mathrm{Im}\left[n_{eff}(\lambda)\right] \tag{12}$$

As we are using $ZnGeP_2$ material, we need to calculate the effective material loss (EML) which is symbolized as α_{eff} and can be computed from the following equation,

$$\alpha eff = \frac{\sqrt{\epsilon_0/\mu_0}\left(\int \left(n\alpha_{mat}|E|^2 dA\right)\right)}{2\int S_z dA} = \alpha_{mat}\eta \tag{13}$$

Here, the integral part of the denominator covers the whole region of the proposed PCF whereas the numerator indicates the $ZnGeP_2$ region. The μ_0 and ε_0 denotes the permeability and permittivity at free space respectively.

4. Optical characteristics aligned with the dynamics of supercontinuum generation

Our proposed PCF is structured in such a way that the desired optical features can be achievable for attaining wide SC. We have engineered the fiber and ZDW is achieved at 2200 nm. Fig. 2 (a) and 2 (b) represents nonlinearity and dispersion characteristics respectively over 2000–3000 nm wavelength. Air hole diameter, $d = 2$ μm is considered for all the layers. Adjacent air holes in between distance from center named as pitch is considered as, $\Lambda = 3$ μm. The dispersion is engineered and optimized at $d = 0.4\Lambda$.

Employing FEM, refractive index as a function of wavelength of $ZnGeP_2$ are estimated and projected in Fig. 2(a). The refractive index of our proposed material is good enough over the selected wavelength span. With rise in wavelength, light spread outside and effective area get increased accordingly. Therefore nonlinearity maintains decreasing nature accordingly which is illustrated in the figure.

According to Eqs. (12) and (13) we calculated the fiber losses as of CL and EML for the optimized condition with ±2 % variation that signifies the robustness of design. Fig. 3 (a) exposes low confinement loss as of 8.437×10^{-9} dB/m and Fig. 3 (b) reveals EML as low as 0.00935 dB/m.

Finally, the optical properties achieved has been summarized and compared with the published researches in Table 1 as follows.

In this part, our inspection regarding octave spanned SC generation will be demonstrated. For this, we have investigated numerically the evolution and propagation of the short pulse by solving GNLSE (Eq. (2)) through SSFM method. A short pulse having 20 fs width is considered with 2230 nm pump wavelength. The wavelength is chosen such that it maintains the vicinity to ZDW and being in the anomalous regime. Then the pulse is transmitted through 1 mm long fiber for diverse peak power of 1 kW, 3 kW and 5 kW. In this study, fiber losses have been neglected and both frequency and time domain analysis have been performed to reveal the nature of the propagated pulse. Detailed progression of supercontinua can be observed from Fig. 4 (a), 4 (b) and 4 (c).

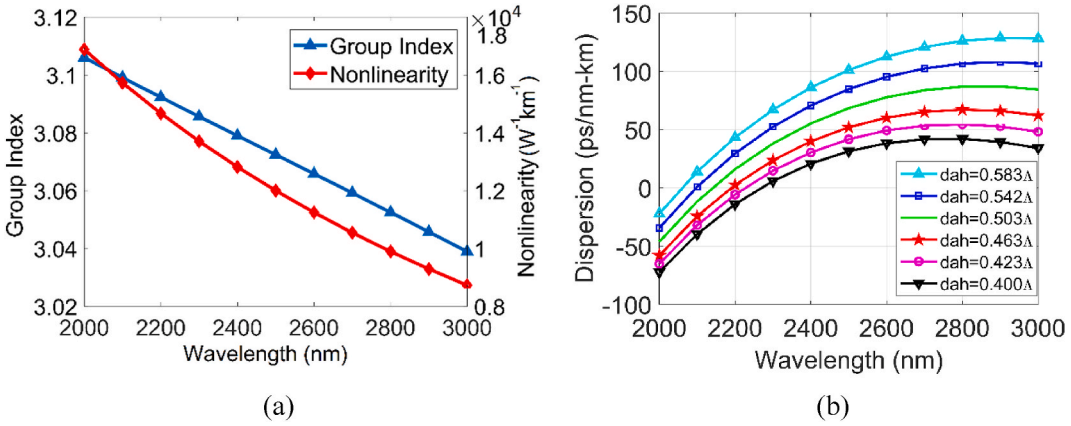

Fig. 2. (a) Refractive index variation of different materials in comparison to our proposed material ($ZnGeP_2$) figured from Sellmeier's equation, (b) various air hole diameter based dispersion sketch of the fiber at 2000–3000 nm. ZDW shifts right with diameter reduction of air hole. Based upon the ZDW location, the proposed PCF is optimized at pitch, $\Lambda = 3$ μm and $d = 0.4\Lambda$. Remarkable nonlinearity near ZDW, helps to generate broadened supercontinuum spectrum.

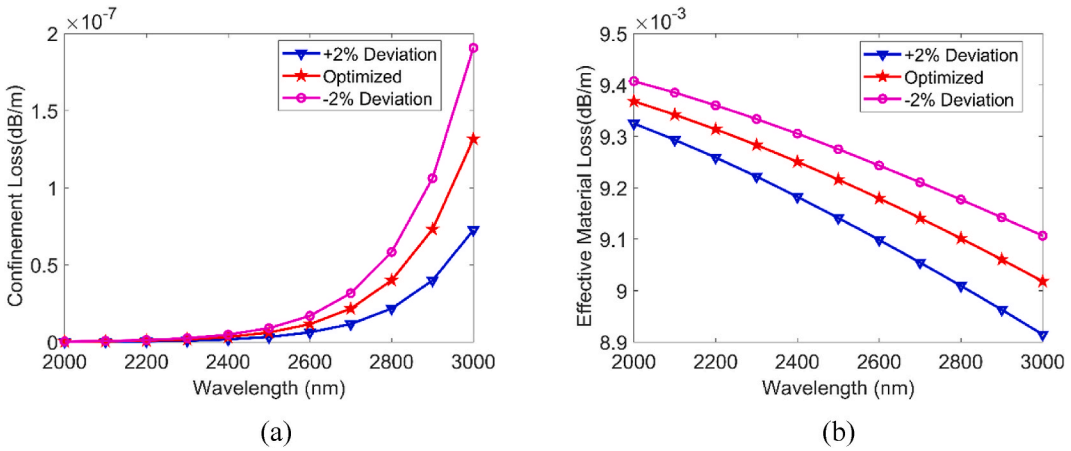

Fig. 3. (a) Confinement loss and (b) Effective material loss at optimized fiber condition (pitch, $\Lambda = 3$ μm and $d = 0.4\Lambda$) with ±2 % variation.

Table 1
Comparison of various optical features exposed by our proposed PCF with earlier studies Conducted.

Ref.	Year of Publication	Material used	CL (dB/m)	EML (dB/m)	Nonlinearity ($W^{-1}km^{-1}$)	Operating Wavelength (nm)
[15]	2021	As_2S_3	9×10^{-8}	0.023	20,268	1550
[22]	2020	Borosilicate	–	–	2300	2500
[23]	2021	Si	–	–	5500	2460
[25]	2019	Si_3N_4	–	–	400	1550
[30]	2020	CCl4	–	–	1190	1550
[31]	2023	$ZnGeP_2$	1.11×10^{-9}	–	13,355	2225
This study	–	$ZnGeP_2$	8.43×10^{-9}	0.00935	14,370	2200

Prior understanding dynamics of SC, we need to understand ultrashort pulse transmission technique through PCF. Short optical pulse forms soliton by balancing dispersion with self-phase modulation (SPM) in anomalous dispersion regime and remains unchanged with respect to wavelength change. With rise in peak power, various nonlinear effect (self-steepening, modulation instability, stimulated Raman scattering etc.) becomes visible and fundamental soliton is generated from higher-order soliton breaking. Later to this soliton breaking, dispersive wave generation happened from the rest of the energy of higher-order soliton and fundamental soliton shifts to lengthier wavelengths. At the same time, dispersive radiation causes blue shift (shift to shorter wavelengths) to the spectrum and accordingly a broader continuum is generated which is the desired SC spectrum.

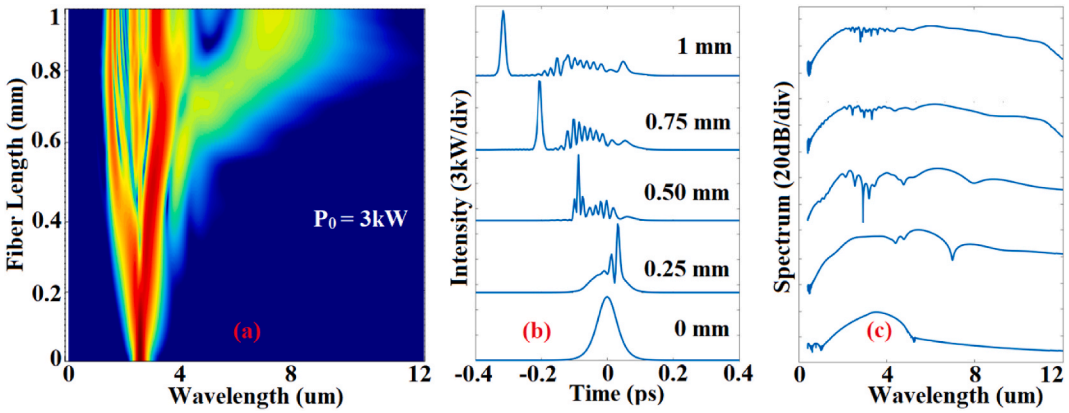

Fig. 4. (a) Surface plot of supercontinuum in 1 mm long single material fiber with peak power of 3 kW, corresponding (b) temporal and (c) spectral plot at center wavelength of 2230 nm.

From Fig. 4 (a), it is clear that At 3 kW, the progression of the spectrum towards lengthier wavelengths becomes much more pronounced. Up to 0.25 mm fiber length, the soliton maintains its nature and then pulse breaking starts which can be observed from Fig. 4 (b). It is also evident that the Raman effect come into the scenario at 0.5 mm propagation length. After that a continuous shift can be observed from the temporal figure up to 1 mm fiber length. Corresponding spectral changes can be observed from Fig. 4 (c).

Fig. 5 reveals the spectral intensity profile at 2230 nm pump wavelength for various peak power. Intensity profile of generated spectrum for 1 kW, 3 kW and 5 kW peak power are demonstrated in Fig. 5 (a), 5 (b) and 5 (c) respectively. There is no separated wave peaks in the prevailing's of ZDW line. The blue shift can substantially be witnessed from Fig. 5 (b) due to increase in power as 3 kW. Moreover, Raman induced energy transfer is relatively higher which is evident in Fig. 5. For achieving wide SC spectra there should be made a balance of improved nonlinearity and tuned dispersion nearer ZDW. Accordingly, over five octave spanning SC has been obtained at 2230 nm wavelength with a combination of 5 kW peak power. The spectrum spanned around 33,000 nm and exposed in Fig. 5 (c). This much spanning is attained because of choosing the pump wavelength at 2230 nm which is very nearer to ZDW and high nonlinearity at that wavelength. The spectra covers 33,000 nm which is more than five octave. Such five octave spanned SC spectra are yet to be proposed for 1 mm long single material fiber according to the best of our knowledge.

At the same time the significant impact of varying pulse width can also be observed from the same figure. The input is altered as 20 fs, 40 fs and 60 fs for simultaneous variation of power as 1 kW, 3 kW and 5 kW. Unlike spectral progression, no spectral gap and dispersive peaks are seen around ZDW line. Increasing input pulse width limits the spanning of SC spectra because of the dominant nature of modulation instability. Rise in pulse width causes increased dispersion length and reduced fission length. Consequently modulation instability get dominant over soliton fission and yields less spanned SC generation. The bandwidths are truncated by – 40 dB.

Lastly, the degree of coherence have been investigated as [32] and revealed in Fig. 5. Quantum noise is considered in this particular case. Fig. 6 clearly indicates that reasonably better coherence observed at 5 kW in pump wavelength of 2230 nm. Table 2 summarizes a comparison of SC achieved in case of proposed PCF with previously published research work.

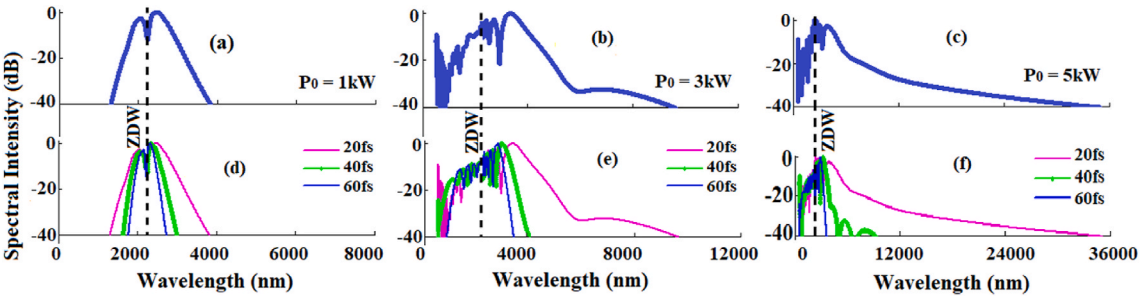

Fig. 5. Spectral intensity of supercontinuum in 1 mm long single material fiber with peak power of 1 kW (a), 3 kW (b) and 5 kW (c) at center wavelength of 2230 nm. Intensity variation depending upon various input pulse width with peak power of 1 kW (d), 3 kW (e) and 5 kW (f).

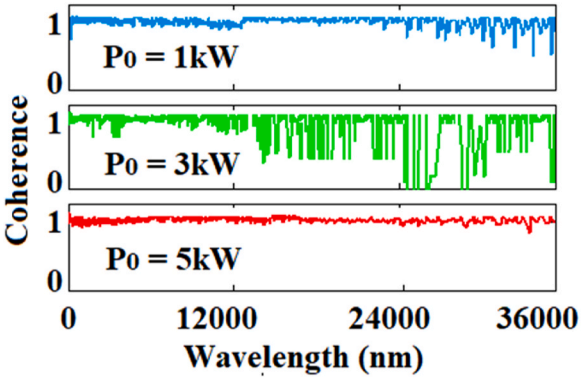

Fig. 6. 2230 nm pump wavelength based coherence plot for 1 kW, 3 kW and 5 kW.

Table 2
SC achieved in Contrast to other published research.

Researches	Materials	Fiber length (mm)	Peak Power (kW)	SC Span (nm)
[15]	As_2S_3	1	3	11,454
[11]	GAP-Se	10	0.95	9000
[33]	GeAsSeTe	200	5	9600
[23]	Si	10	1	2700
[34]	$Ga_8Sb_{32}S_{60}$	10	20	7590
[26]	SiN	2	0.05	6300
[22]	Borosilicate glass	100	0.35	2100
[25]	Si_3N_4	10	5	5700
[31]	$ZnGeP_2$	1	5	31,000
This study	$ZnGeP_2$	1	5	33,000

5. Conclusion

In summary, a $ZnGeP_2$ material based PCF has been proposed for more than five octave spanning SC generation. The designed and proposed structure projects ZDW at 2200 nm, nonlinearity as 14,370 $W^{-1}km^{-1}$ and confinement loss as 8.43×10^{-09} dB/m. Our single material structure generated over five octave spanning SC (around 33,000 nm) in very short length as of 1 mm. The input is considered as 20 fs at 5 kW power and pumped at 2230 nm. $ZnGeP_2$ material with such exceptional optical characteristics for more than five octave spanned SC generation can play a vital role in different laser applications.

Data availability statement

Data will be made available on request.

CRediT authorship contribution statement

Shah Md Salimullah: Writing – original draft, Validation, Software, Methodology, Investigation, Formal analysis, Data curation, Conceptualization. **Mohammad Faisal:** Writing – review & editing, Visualization, Supervision.

Declaration of competing interest

The authors declare that they have no known competing financial interests or personal relationships that could have appeared to influence the work reported in this paper.

References

[1] R.R. Alfano, S.L. Shapiro, Observation of self-phase modulation and small-scale filaments in crystals and glasses, Phys. Rev. Lett. 24 (11) (1970) 592.
[2] S.V. Smirnov, J.D. Ania-Castañón, S. Kobtsev, S.K. Turitsyn, Supercontinuum in telecom applications, in: The Supercontinuum Laser Source, Springer, 2016, pp. 371–403.

[3] K.F. Lee, A. Rolland, P. Li, J. Jiang, M.E. Fermann, Supercontinuum optimization at six spectral lines for frequency metrology using phase shaping, in: Nonlinear Frequency Generation and Conversion: Materials and Devices XXI, SPIE, 2022, pp. 43–47.
[4] R. Krebbers, et al., Mid-infrared supercontinuum-based fourier transform spectroscopy for plasma analysis, Sci. Rep. 12 (1) (2022) 1–11.
[5] S. Rao Ds, et al., Shot-noise limited, supercontinuum-based optical coherence tomography, Light Sci. Appl. 10 (1) (2021) 1–13.
[6] Y. Cheng, et al., Mid-infrared supercontinuum and frequency comb generations by different optical modes in a multimode chalcogenide strip waveguide, IEEE Access 8 (2020) 202022–202031.
[7] C. Poudel, C.F. Kaminski, Supercontinuum radiation in fluorescence microscopy and biomedical imaging applications, JOSA B 36 (2) (2019) A139–A153.
[8] W. Bi, J. Gao, X. Li, L. Xiong, M. Liao, Mid-infrared supercontinuum generation in silica photonic crystal fibers, Appl. Opt. 55 (23) (Aug. 2016) 6355–6362, https://doi.org/10.1364/AO.55.006355.
[9] A. Medjouri, E.-B. Meraghni, H. Hathroubi, D. Abed, L.M. Simohamed, O. Ziane, Design of ZBLAN photonic crystal fiber with nearly zero ultra-flattened chromatic dispersion for supercontinuum generation, Optik 135 (Apr. 2017) 417–425, https://doi.org/10.1016/j.ijleo.2017.01.082.
[10] W. Geng, et al., 1.6-Octave coherent OAM supercontinuum generation in As2S3 photonic crystal fiber, IEEE Access 8 (2020) 168177–168185, https://doi.org/10.1109/ACCESS.2020.3023133.
[11] P. Chauhan, A. Kumar, Y. Kalra, Numerical exploration of coherent supercontinuum generation in multicomponent GeSe2-As2Se3-PbSe chalcogenide based photonic crystal fiber, Opt. Fiber Technol. 54 (Jan. 2020) 102100, https://doi.org/10.1016/j.yofte.2019.102100.
[12] W. Gao, et al., Mid-infrared supercontinuum generation in a suspended-core As2S3 chalcogenide microstructured optical fiber, Opt Express 21 (8) (Apr. 2013) 9573–9583, https://doi.org/10.1364/OE.21.009573.
[13] S. Hossain, S. Shah, M. Faisal, Ultra-high birefringent, highly nonlinear Ge20Sb15Se65 chalcogenide glass photonic crystal fiber with zero dispersion wavelength for mid-infrared applications, Optik 225 (Jan. 2021) 165753, https://doi.org/10.1016/j.ijleo.2020.165753.
[14] R. Sharma, S. Kaur, P. Chauhan, A. Kumar, Computational design & analysis of GeSe2-As2Se3-PbSe based rib waveguide for mid-infrared supercontinuum generation, Optik 220 (Oct. 2020) 165032, https://doi.org/10.1016/j.ijleo.2020.165032.
[15] S.M. Salimullah, M.S. Hossain, M. Faisal, Efficient and wide supercontinuum generation in dispersion engineered tellurite clad As2S3 core photonic crystal fiber within 1 mm of fiber length, Opt. Eng. 60 (6) (Jun. 2021) 066110, https://doi.org/10.1117/1.OE.60.6.066110.
[16] Y.O. Azabi, A. Agrawal, N. Kejalakshmy, B.M.A. Rahman, K.T.V. Grattan, Equiangular spiral tellurite photonic crystal fiber for supercontinuum generation in mid-infrared, in: CLEO:2011 - Laser Applications to Photonic Applications (2011, Optical Society of America, May 2011, p. JThB72, https://doi.org/10.1364/CLEO_AT.2011.JThB72, paper JThB72.
[17] G.A. Verozubova, A.I. Gribenyukov, V.V. Korotkova, O. Semchinova, D. Uffmann, Synthesis and growth of ZnGeP2 crystals for nonlinear optical applications, J. Cryst. Growth 213 (3) (Jun. 2000) 334–339, https://doi.org/10.1016/S0022-0248(00)00362-6.
[18] S. Das, G.C. Bhar, S. Gangopadhyay, C. Ghosh, Linear and nonlinear optical properties of ZnGeP2 crystal for infrared laser device applications: revisited, Appl. Opt. 42 (21) (Jul. 2003) 4335–4340, https://doi.org/10.1364/AO.42.004335.
[19] V.P. F. Rotermund F. Noack, P. Schunemann, Characterization of ZnGeP2 for parametric generation with near-infrared femtosecond pumping, Fiber Integrated Opt. 20 (2) (Mar. 2001) 139–150, https://doi.org/10.1080/01468030121384.
[20] A.N. Ghosh, M. Klimczak, R. Buczynski, J.M. Dudley, T. Sylvestre, Supercontinuum generation in heavy-metal oxide glass based suspended-core photonic crystal fibers, JOSA B 35 (9) (Sep. 2018) 2311–2316, https://doi.org/10.1364/JOSAB.35.002311.
[21] M. Klimczak, et al., Mid-infrared supercontinuum generation in soft-glass suspended core photonic crystal fiber, Opt. Quant. Electron. 46 (4) (Apr. 2014) 563–571, https://doi.org/10.1007/s11082-013-9802-1.
[22] S. Kalra, et al., Investigation of As2S3-borosilicate chalcogenide glass-based dispersion-engineered photonic crystal fibre for broadband supercontinuum generation in the mid-IR region, J. Mod. Opt. 67 (10) (Jun. 2020) 920–926, https://doi.org/10.1080/09500340.2020.1788658.
[23] Z. Dashtban, M.R. Salehi, E. Abiri, Supercontinuum generation in near- and mid-infrared spectral region using highly nonlinear silicon-core photonic crystal fiber for sensing applications, Photon. Nanostruct: Fundam. Appl. 46 (Sep. 2021) 100942, https://doi.org/10.1016/j.photonics.2021.100942.
[24] Z. Hui, L. Zhang, W. Zhang, CMOS compatible on-chip telecom-band to mid-infrared supercontinuum generation in dispersion-engineered reverse strip/slot hybrid Si3N4 waveguide, J. Mod. Opt. 65 (1) (Jan. 2018) 53–63, https://doi.org/10.1080/09500340.2017.1376718.
[25] H. Ahmad, M.R. Karim, B.M.A. Rahman, Dispersion-engineered silicon nitride waveguides for mid-infrared supercontinuum generation covering the wavelength range 0.8–6.5 μ m, Laser Phys. 29 (2) (Feb. 2019) 025301, https://doi.org/10.1088/1555-6611/aaf63d.
[26] M.R. Karim, N. Al Kayed, N. Jahan, M.S. Alam, B.M.A. Rahman, Study of highly coherent mid-infrared supercontinuum generation in CMOS compatible Si-rich SiN tapered waveguide, J. Lightwave Technol. 40 (13) (2022) 4300–4310.
[27] A. Hartung, J. Bierlich, A. Lorenz, J. Kobelke, M. Jäger, Design and fabrication of all-normal dispersion nanohole suspended-core fibers, JOSA B 36 (12) (Dec. 2019) 3404–3410, https://doi.org/10.1364/JOSAB.36.003404.
[28] I.A. Sukhoivanov, S.O. Iakushev, O.V. Shulika, J.A. Andrade-Lucio, A. Díez, M. Andrés, Supercontinuum generation at 800 nm in all-normal dispersion photonic crystal fiber, Opt Express 22 (24) (Dec. 2014) 30234–30250, https://doi.org/10.1364/OE.22.030234.
[29] M.R. Karim, B.M.A. Rahman, G.P. Agrawal, Dispersion engineered Ge 11.5 as 24 Se 64.5 nanowire for supercontinuum generation: a parametric study, Opt Express 22 (25) (2014) 31029–31040.
[30] A. Sharafali, K. Nithyanandan, A theoretical study on the supercontinuum generation in a novel suspended liquid core photonic crystal fiber, Appl. Phys. B 126 (4) (2020) 55.
[31] S.M. Salimullah, M. Faisal, Ultra-wideband and coherent supercontinuum generation (near and mid-infrared) in dispersion flattened ZnGeP2 photonic crystal fiber, Alex. Eng. J. 70 (2023) 289–300.
[32] J.M. Dudley, G. Genty, S. Coen, Supercontinuum generation in photonic crystal fiber, Rev. Mod. Phys. 78 (4) (2006) 1135.
[33] B. Wu, et al., Mid-infrared supercontinuum generation in a suspended-core tellurium-based chalcogenide fiber, Opt. Mater. Express 8 (5) (May 2018) 1341–1348, https://doi.org/10.1364/OME.8.001341.
[34] A. Medjouri, D. Abed, Z. Becer, Numerical investigation of a broadband coherent supercontinuum generation in Ga8Sb32S60 chalcogenide photonic crystal fiber with all-normal dispersion, Opto-Electron. Rev. 27 (1) (2019) 1–9.